Extrusion of Ingot and Powder Metallurgy Aluminum Matrix Composites Profiles

Marcela Lieblich, Gaspar González-Doncel, Joaquín Ibáñez, Ricardo Fernández, VirginiaVadilo, *CENIM-CSIC*, Madrid, Spain

Pilar Rey, Alfonso Vázquez, Gemma Castro, *AIMEN*, Porriño, Spain

Several profiles with the same extrusion ratio were extruded from three monolithic alloys and five aluminum matrix composites (AMCs) prepared by ingot and powder metallurgy (PM). Specifically, AA6061 and AA6063 were reinforced by 10 and 25 vol.% of Al_2O_3 and $MoSi_2$ intermetallic particles. To study the wear of the dies, high temperature pin-on-disk tests were performed. The results show that the composite profiles present high surface and dimensional quality and that the die steel wears slightly more against the cast composite. Maximum extrusion pressure (Pmax) depends on profile shape and increases in the following order: bar, T, L and U, and tube. It also increases as volume fraction of reinforcement increases. In general, cast materials are easier to extrude than PM ones, and $MoSi_2$ reinforced AMCs are easier to extrude than Al_2O_3 ones. AMCs processed by PM have significantly higher hardness than the cast AMC and the monolithic alloys. The PM composites do not need any heat treatment to acquire maximum hardness. By adding reinforcing particles to aluminum, a significant increase in tensile strength and stiffness occur. The high tensile strength and modulus of the present PM composites, without a decrease in specific properties, makes these AMCs interesting for structural applications.

INTRODUCTION

Particle-reinforced aluminum matrix composites (AMCs) are of considerable interest as structural materials due to their high stiffness and strength to weight ratio and isotropic properties, which are superior in general to those of conventional aluminum alloys [Clyne 1993, Chawla 2006]. Brake rotors, pistons, connecting rods and integrally cast AMCs engine blocks are some of the successful applications of these materials in the automotive industry [Prasad 2004, Zebarjad 2007].

The extrusion process extended to AMCs offers profiles with higher stiffness, mechanical strength, and wear resistance for structural applications, (for example but not exclusively, in the automotive and aerospace industries) in the replacement of iron and titanium base alloys. On the other hand, extrusion parameters are more critical for AMCs than for monolithic alloy matrices [Lieblich 1997] because of the higher flow stress of the former, so that the complexity of profiles may be restricted.

Hard ceramic particles, such as SiC or Al_2O_3, are widely employed as reinforcement of AMCs because of their high hardness and elastic modulus [Chawla 2006]. However, their high abrasiveness complicates the processing and machining steps and severely damages tools. In the last few years, intermetallics have

emerged as possible substitutes for ceramic reinforcement. Among them $MoSi_2$ has proved to be an excellent candidate as it confers high thermal stability and mechanical properties on the AMCs, together with good tribological properties [Corrochano 2009, Corrochano 2011].

Casting methods are commonly employed to produce AMCs. However, during processing by casting the interface between reinforcement and matrix may become altered by diffusion reaction products that arise because of the high temperatures involved, and more often than not these are deleterious. In addition, a uniform distribution of reinforcement particles, which is a prime requisite for obtaining a reliable material, is hardly achieved by the liquid route, especially for small reinforcing size.

Powder metallurgy (PM) is an important processing technique for producing AMCs that can eliminate diffusion reaction products and reinforcement agglomeration that typically occur in the casting metallurgy process. However, clustering may still occur because of static charges acting on particle surfaces, or due to geometrical constraints when there is a large difference between matrix and reinforcing particle sizes [Tan 1998]. Ball milling is commonly used to overcome this problem because it improves particle distribution [Lu 1998, Parvin 2008, Murphy 1998, Boey 1998, Liu 1993, Prebhu 2006, Fogagnolo 2006, Ozdemir 2008, Zhao 2005, Lu 2000]. This is due to the process that the aluminum particles are forced to undergo, i.e. deformation, fracturing and cold welding; and the harder reinforcing particles, i.e. fracturing, with the final result of fine reinforcing particles becoming well embedded into the aluminum matrix. In addition, ball milling is also well known because it reduces aluminum grain size and promotes the incorporation of an extremely fine distribution of oxide dispersoids in the alloy matrix. All these features increase the mechanical response of the composite material without a significant loss of ductility [Corrochano 2011].

In the present work, several metal matrix composites have been extruded employing different profiles. More specifically, three aluminum matrices have been selected that have been reinforced by 10 or 25vol.% of Al_2O_3 or $MoSi_2$ particles, either by a ingot (AA6061) or a powder metallurgy (AA6061 and AA6063) route that includes ball milling. At least three H13 steel dies were employed with each material that produced cylindrical bars, L profiles and rectangular tubes, all of them with the same extrusion ratio. The purpose of this paper is to investigate the effect of reinforcement type and volume fraction on the extrudate properties, depending on the processing route and the alloy matrix. Another important factor that was considered is the wear of the dies. To study this aspect, wear was simulated from high temperature pin-on-disk tests. The results were compared with those of the monolithic alloy matrices, processed following the same protocol.

EXPERIMENTAL PROCEDURE

A horizontal lab-scale computerized extrusion press, 300 ton capacity, was used for this work, Figure 1. Ram speed can be varied between 0.3 and 12 mm/s. The extrusion container, of 44 mm diameter, can be heated up to 500ºC. Extrusion pressures as high as 1700 MPa can be reached.

Three aluminum alloys have been employed as reference monolithic materials: 6082 ingot as a bar of 42 mm in diameter, and 6061 and 6063 as powder batches with particle diameter < 50 μm supplied by Alpoco, Sutton Coldfield, UK. Table 1 shows the nominal composition of these alloys. For the cast composite, 6061/Al_2O_3/10p material with median Al_2O_3 diameter of 10 μm was acquired from QED Extrusion Developments Inc., San Diego, USA, in extruded bars of 62 mm diameter which were machined to 42 mm to fit into the extrusion container. The composites processed by powder metallurgy were reinforced either with Al_2O_3 particles of 14 to 20 μm in size or with $MoSi_2$ particles of 10 to 40 μm in size, the latter were obtained by self-propagating high temperature synthesis at Tecnalia, San Sebastian, Spain. Two reinforcement volume fractions were selected: 10 and 25%. Mixing was carried out by planetary ball milling operating at 200 rpm with a ratio of balls to material of 7:1 for 10 hours without process agent control. During the ball milling, fragile particles normally break whereas ductile particles deform

plastically. The powders were encapsulated in 6063 cans and consolidation was achieved during the extrusion process.

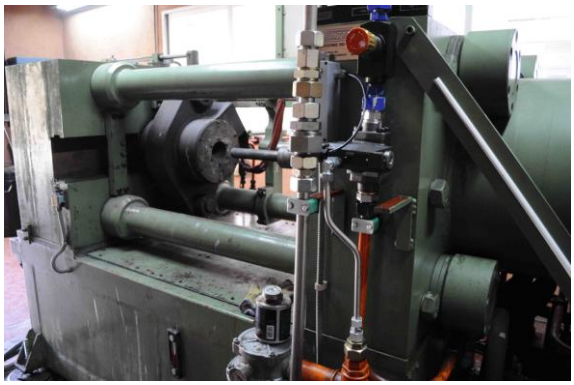

Figure 1. Lab-scale extrusion press at CENIM-CSIC.

Table 1. Nominal composition of the aluminum alloys employed (mass %)

Alloy	**Mg**	**Si**	**Fe**	**Cu**	**Mn**	**Cr**	**Zn**	**Ti**	**Other**	**Al**
6082	0.6-1.2	0.7-1.3	0.50	0.10	0.40-1	0.25	0.20	0.10	0.15	Bal.
6061	0.8-1.2	0.4-0.8	0.7	0.15-0.4	0.15	0.04-0.35	0.25	0.15	0.15	Bal.
6063	0.45-0.9	0.2-0.6	0.35	0.10	0.10	0.10	0.10	0.10	0.15	Bal.

All extrusions were conducted at a temperature of 450ºC, an extrusion ratio of 37:1 and a ram speed of 2 mm/s, equivalent to an extrusion velocity of 74 mm/s. Five profiles were extruded. Dies were supplied by Iberia Dies Phoenix, Zaragoza, Spain: circular of 7.2 mm diameter, L of 17.7 mm length and 1.2 mm width, U of 17.7 mm length and 0.8 mm width, a rail type called T from now on, and a rectangular tube of 10.1 x 8.1 mm and 1.2 mm wall thickness, Figure 2. The extruded profiles were left to air cool. Table 2 lists all the materials prepared and their codes.

Table 2. Investigated materials, processing routes, profiles and codes.

Material/Code	**Matrix**	**Reinforcement**	**Vol. %**	**Processing route**	**Profile**
6082_C	6082	-	-	Casting	● L ☐ U T
6061_PM	6061	-	-	Powder Metallurgy	● L ☐
6063_PM	6063	-	-	Powder Metallurgy	● L ☐
6061/Al_2O_3/10p_C	6061	Al_2O_3	10	Casting	● L ☐ U T
6061/Al_2O_3/10p_PM	6061	Al_2O_3	10	Powder Metallurgy	● L ☐
6061/Al_2O_3/25p_PM	6061	Al_2O_3	25	Powder Metallurgy	● L ☐
6063/Al_2O_3/25p_PM	6063	Al_2O_3	25	Powder Metallurgy	● L ☐
6061/$MoSi_2$/25p_PM	6061	$MoSi_2$	25	Powder Metallurgy	● L ☐

Several characteristics were investigated in some or all of the extruded profiles with the aim of studying the influence of processing route, volume fraction and type of reinforcement on the composite properties. These are: maximum extrusion pressure (Pmax), microstructure, hardness, yield stress ($\sigma_{0.2}$), ultimate tensile strength (UTS) and elongation to fracture (A), Young's modulus (E), and wear resistance.

All pressure-displacement curves were recorded during extrusion. Microstructural characterization was performed by optical and scanning electron microscopy (SEM) using a FEG-JEOL 6500 microscope. Vickers hardness of consolidated bars was measured in as-solutionized condition (S) (520ºC for 30 minutes followed by oil quenching and kept in the freezer) and T6 condition (subsequent annealing 24 h at 160ºC). At least 3 indentations were performed for each condition by applying a load of 10 kg for 10 seconds. The results are presented with an accuracy of ± 3%. Tensile tests were performed in a MTS 250 kN on L and U profiles in T6 condition according to UNE-EN ISO 6892-1 with extensometer MTS 632.25F-20.

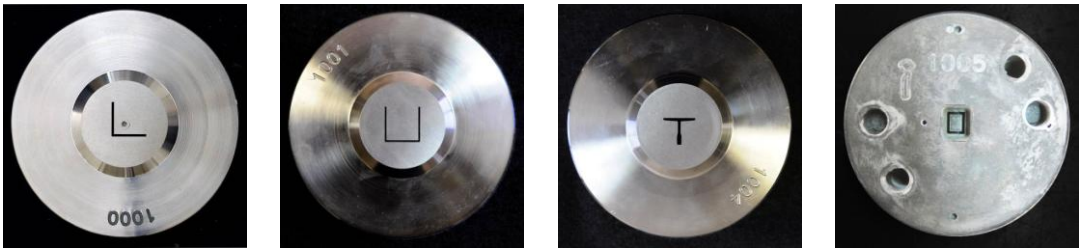

Figure 2. Extrusion dies: L, U, T and □.

Pin-on-disk wear tests were carried against a disk of hardened and tempered H13 steel during 30 minutes. Pins were machined by electrical discharge from the monolithic 6082_C and 6061/Al_2O_3/10p_C composites. Tests conditions were: temperature, 500ºC; applied load, 15 N; angular speed, 50 rpm.; linear speed, 0.063 m/s; number of revolutions: 1500. The material transfered to the tool was studied in the SEM.

RESULTS AND DISCUSSION

The extruded profiles had bright surfaces and correct dimensions, as shown in the examples of Figure 3. The only exception was for the PM AMCs reinforced with Al_2O_3 on which blisters were present. These blisters appeared during extrusion for the tubes, and during solid solution treatment for the L profiles. This defect points to a problem of cleanness of the Al_2O_3 particles, which is a subject of present study.

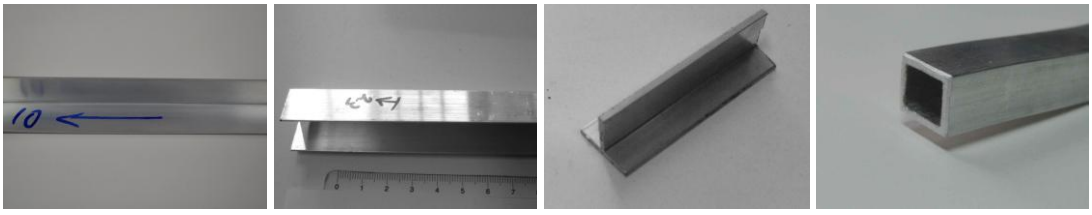

Figure 3. Example of extruded profiles: L, U, T and □.

Extrusion pressure for a given material was different for each profile. Given that all profiles were obtained with the same extrusion ratio, i.e. the same area reduction, other parameters should account for this difference. Figure 4 shows maximum pressure for the five profiles obtained with the monolithic 6082 alloy and the 6061/Al_2O_3/10p_C composite as a function of circumscribed circle diameter. As is evident

from the graph, there is no simple relation between these parameters. The general trend is that maximum pressure increases in the order: bar, T, L and U, and tube, and that the composite needs higher extrusion pressure than the monolithic alloy. The higher Pmax of the tubes may be attributed to a higher energy required for the welding of the two halves of that profile.

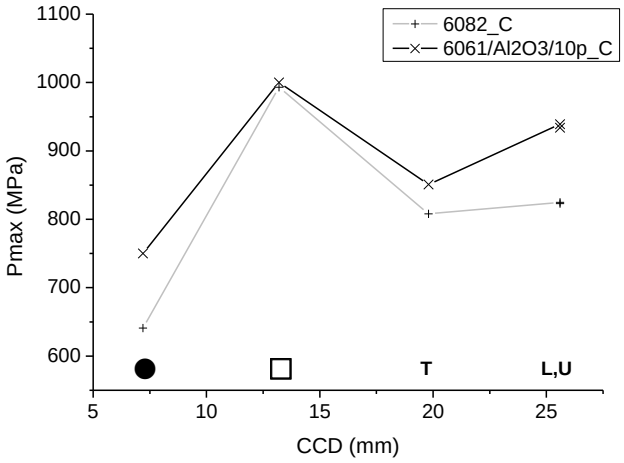

Figure 4. Maximum extrusion pressures (Pmax) as a function of circumscribed circle diameter (CCD) for 6082_C and 6061/Al_2O_3/10p_C materials.

Figure 5 shows a bar diagram of maximum pressure needed to extrude a bar, an L and a tube for the eight materials studied: three monolithic alloys, two AMCs reinforced with 10 vol.% of ceramic particles and three AMCs reinforced with 25 vol.% of ceramic and intermetallic particles. Several factors that illustrate the materials behavior can be deduced from this graph:

- In all cases, maximum pressure increases in the order: bar, L, tube,
- for a given profile, the three unreinforced alloys require roughly the same extrusion pressure, and the 6061_PM material (light magenta columns) is the one that needs a slightly higher Pmax,
- the addition of 10 vol. % of particles by a casting route (dark gray columns) does not make a significant difference in extrusion pressure when compared with the unreinforced alloys,
- the addition of 10 vol. % of particles by a PM route (magenta columns) produces an increase in Pmax only in the case of the tube,
- the addition of 25 vol. % of particles by a PM route (red, blue and olive columns) produces a significant increase in Pmax,
- the use of 6063 alloy matrix (blue columns) instead of 6061(red columns) resulted in a slightly lower Pmax, except for the round bar,
- the use of $MoSi_2$ intermetallic particles (green columns) reduces slightly Pmax with respect to the same AMC reinforced with Al_2O_3,
- as the complexity of the profile increases, the extra pressure needed to extrude the investigated materials was higher for the PM composites than for the monolithic alloys and the cast composite, and increases as the volume fraction of reinforcement increases.

To sum up the results listed above it can be said that, in general, the unreinforced alloys are easier to extrude than the composites, the cast materials are easier to extrude than the PM ones, the $MoSi_2$ reinforced AMCs are easier to extrude than the Al_2O_3 reinforced AMCs, and Pmax increases as volume fraction of reinforcement increases. Although these are in fact the expected trends, the specific values were unknown

until now. This is important because the maximum extrusion pressure is a limiting factor for the introduction of a new material in industrial practice.

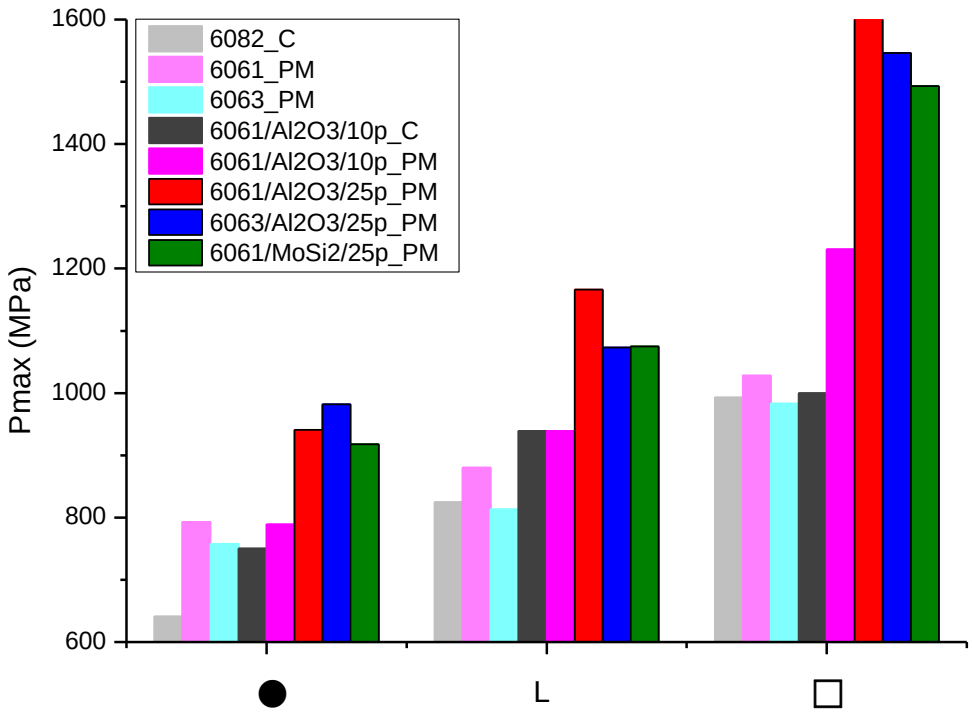

Figure 5. Bar diagram of maximum extrusion pressure (Pmax) as a function of profile type for the eight materials studied.

To compensate for the around 30% increase of extrusion pressure of AMCs with regards to the monolithic alloys, their mechanical properties should increase accordingly. Table 3 shows Vickers hardness of the extruded materials in the as-solutionized (S) and T6 conditions. The unreinforced alloys presented approximately the same hardness, i.e. around 0.65 and 1.10 GPa in S and T6 condition, respectively. The cast AMC 6061/Al_2O_3/10p_C has a similar S hardness but a higher T6 hardness. With regard to the PM composites, their hardness in the S condition is considerably higher than that of the monolithic alloys, which reflects the contribution of the reinforcing particles and the PM route. It is notorious that the PM composites reinforced with 25 vol. % of Al_2O_3 are significantly softer than the same composite reinforced with $MoSi_2$. This may be attributed to the defects that appeared in the ceramic reinforced PM AMCs. In spite of this problem, it is noteworthy that the hardness of these composites in the S condition is as high as the hardness of the corresponding matrix alloy in the T6 condition. When the comparison is made between the intermetallic reinforced AMC 6061/$MoSi_2$/25p_PM and the unreinforced alloys the hardness increase is still more remarkable: almost three times with respect to the S condition and more than 45% higher with respect to the T6 condition. Also worth to notice is the absence of hardening of the PM composites, which implies that in these materials there is no need for a heat treatment to obtain maximum hardness. This behavior has been attributed to the submicrometric grain size that is obtained during the high energy ball mixing [Corrochano 2009].

Tensile test results in T6 condition of L-profiles of the monolithic alloys, the cast composite and the $MoSi_2$ reinforced PM composite are presented in Table 4. Among the unreinforced materials, the best properties are shown by the 6061_PM alloy. Interestingly, both PM alloys have higher Young's modulus

than the cast alloy. The best properties of the PM materials are probably due to the presence of very small Al_2O_3 particles that come from the oxide layer that surrounded each aluminum powder particle, which breaks during the deformation they underwent during extrusion. By adding reinforcing particles to aluminum, a significant increase in tensile strength and stiffness occur, which is graphically shown in Figure 6, where the data for vol. % equal to zero is the average of the values of the three unreinforced alloys. Even though elongation to fracture diminishes accordingly, the high tensile strength and modulus, without a decrease in specific properties, makes these AMCs interesting for structural applications. In Table 4, data of tensile results of U-profiles of cast materials are also listed. Whereas UTS, $\sigma_{0.2}$, and A seem independent of the profile shape, the Young´s modulus seems to be slightly higher for the U-profile.

Table 3. Vickers hardness of extruded bars in as-solutionized (S) and T6 conditions

Material	**Hardness (GPa)**	
	S	**T6**
6082_C	0.65	1.08
6061_PM	0.65	1.13
6063_PM	0.61	1.02
6061/Al_2O_3/10p_C	0.56	1.38
6061/Al_2O_3/10p_PM	0.92	0.93
6061/Al_2O_3/25p_PM	1.29	1.28
6063/Al_2O_3/25p_PM	1.08	1.06
6061/$MoSi_2$/25p_PM	1.71	1.66

Table 4. Maximum tensile stress (UTS), yield stress ($\sigma_{0.2}$), elongation to fracture (A) and Young's modulus (E) of selected extrudates in T6.

Material	**Profile**	**UTS (MPa)** ±3%	**$\sigma_{0.2}$ (MPa)** ±5.3 %	**A (%)** ±12.8 %	**E (GPa)** ±3.0%
6082_C	L	305	290	10	65.5
6061_PM	L	348	313	11	73.9
6063_PM	L	294	267	12	72.9
6061/Al_2O_3/10p_C	L	340	309	7	80.7
6061/$MoSi_2$/25p_PM	L	461	379	2	99.0
6082_C	U	310	290	9	69.7
6061/Al_2O_3/10p_C	U	339	308	6	85.1

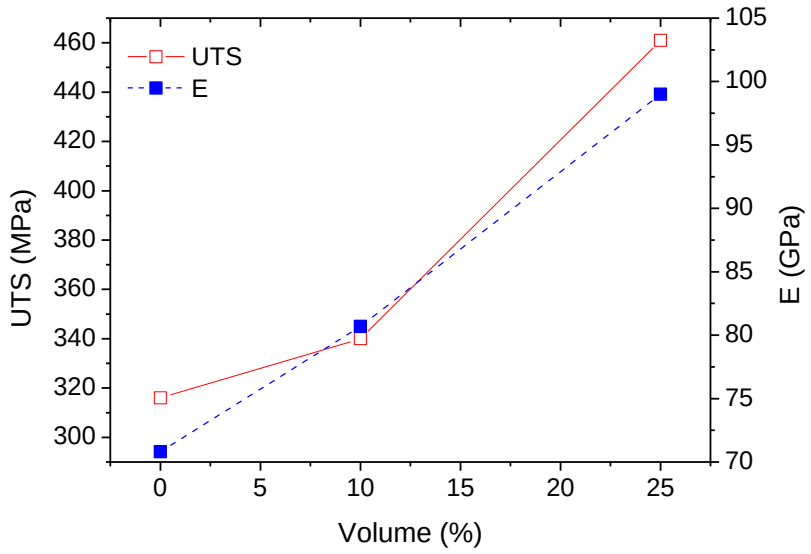

Figure 6. Ultimate tensile strength (UTS) and Young's modulus (E) of L-profiles as a function of volume content of reinforcement.

Metallographic cross sections of the tubes obtained with the AMCs are shown in Figure 7. Although the deformation of the tube walls was not evident in the cast 6061/Al_2O_3/10p_C composite, upon mounting it in Bakelite, the walls appeared curved. In the case of the Al_2O_3 reinforced composites, the defects that were visible in the profiles are also present in the cross sections (arrowed). On the contrary, the $MoSi_2$ reinforced composite profile appears quite free of defects. The darker areas that can be seen in the side walls of the tubes in the PM materials come from the 6063 can, in which the AMC powders were encapsulated and reflect the material flow during the extrusion.

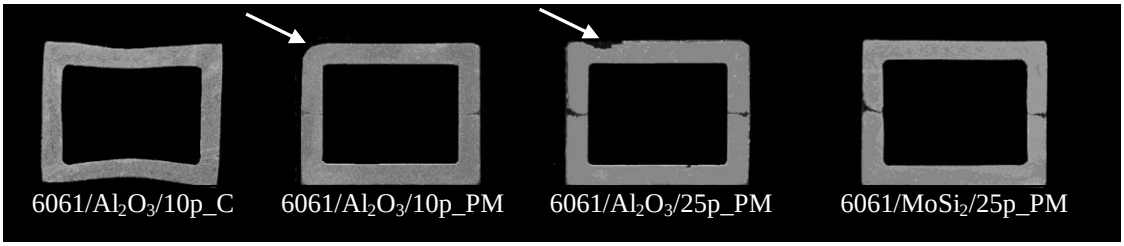

Figure 7. Scanned images of polished cross sections of composite tubes. From left to right: 6061/Al_2O_3/10p_C, 6061/Al_2O_3/10p_PM, 6061/Al_2O_3/25p_PM, 6061/$MoSi_2$/25p_PM

The mechanical response of a composite is highly sensitive to the processing conditions. In fact, it is commonly noted in the literature that there are disagreements over the mechanical properties of composites which are nominally identical to each other but differ in the history of preparation [Borrego 2002]. Thus, optimization of mechanical properties of AMCs can be achieved by adjusting their microstructure, and specifically, of the size and the homogeneity of distribution of reinforcing particles. In general, the smaller and the more homogeneously distributed the particles are, the better the mechanical properties. Figure 8

presents SEM micrographs of tube cross sections corresponding to the cast and PM composites reinforced with 10 vol. % of Al_2O_3, and the 6061 matrix AMCs reinforced with 25 vol. % of Al_2O_3 and $MoSi_2$. From the comparison of the two processing routes it follows that the PM material presents a larger amount of smaller particles. More difficult is to compare the two AMCs reinforced with 25 vol. % and image analyses is in progress to quantify the reinforcement size and the degree of particle clustering.

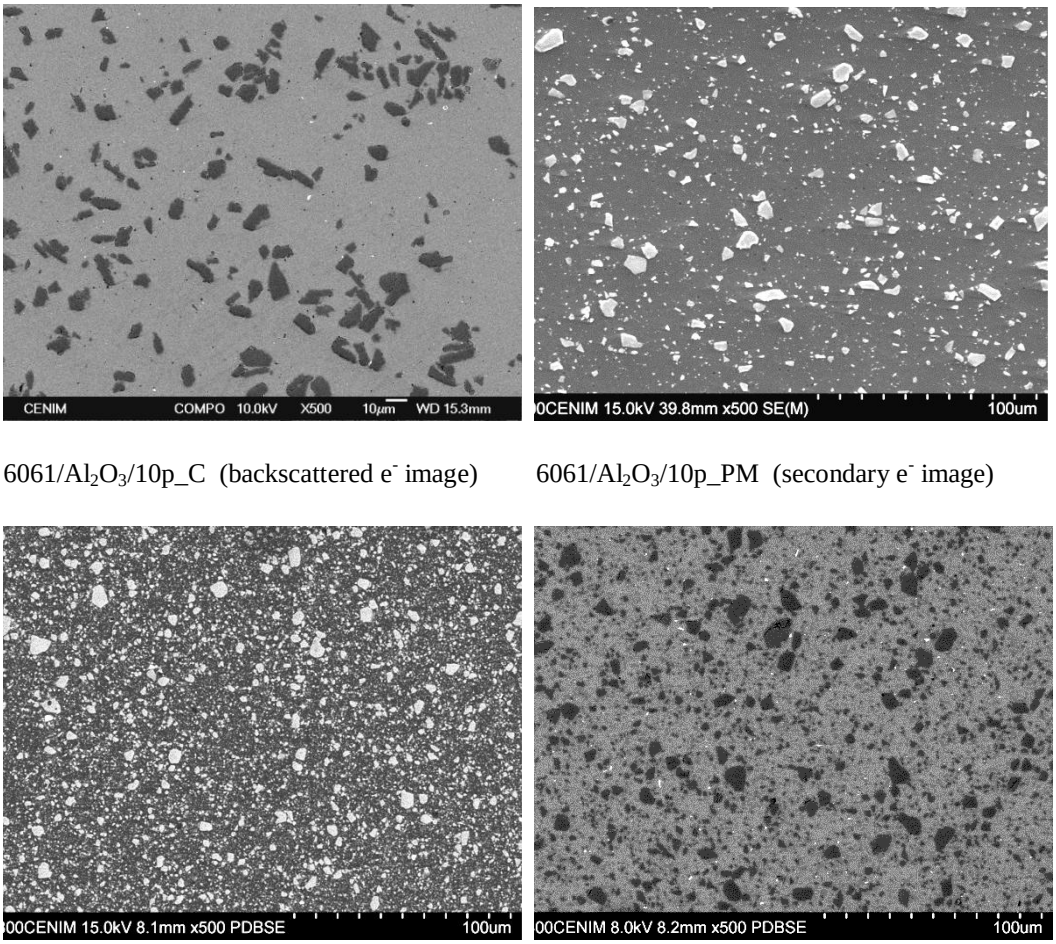

6061/Al_2O_3/10p_C (backscattered e^- image) 6061/Al_2O_3/10p_PM (secondary e^- image)

6061/$MoSi_2$/25p_PM (secondary e^- image) 6061/Al_2O_3/25p_PM (backscattered e^- image)

Figure 8. SEM micrographs of cross sections of 6061/Al_2O_3/10p_C (upper left), 6061/Al_2O_3/10p_PM (upper right), 6061/$MoSi_2$/25p_PM (bottom left) and 6061/Al_2O_3/25p_PM (bottom right) tubes

The objective of the wear tests was to investigate the influence of the ceramic particles on the wear of steel by galling (transfer of aluminum to the tool surface) and abrasion of the steel. SEM micrographs revealed that in all samples aluminum and reinforced aluminum are adhered on the steel surface. On the other hand, steel debris appeared on the pin surfaces. In each of the samples two distinctive wear mechanisms were identified: adhesive and abrasive wear. Concerning the 6082_C pin, the surface oxide film broke down, abrading the steel surface at a fast rate. However, we also have to consider the oxidation of the steel tool. Iron oxide derived from available oxygen can dramatically accelerate wear. Figure 9 a) shows an example of steel debris on the pin surface. In Figure 9b) it can be observed that the surface of the

steel shows not only adhered aluminum but also some grooves as a consequence of abrasive wear. This pin suffered a weight loss of 2 mg. Regarding the 6061/Al_2O_3/10p_C composite, wear of the steel surface resulted a little higher, and again, there were observed the same wear mechanisms as for the unreinforced alloy together with transfer of material between pin and steel counterface. The quantity of transferred material was higher for the reinforced alloy, as can be seen in Figure 10. In this case wear loss was of 6.45 mg, which is a consequence of the presence of the abrasive reinforcement particle.

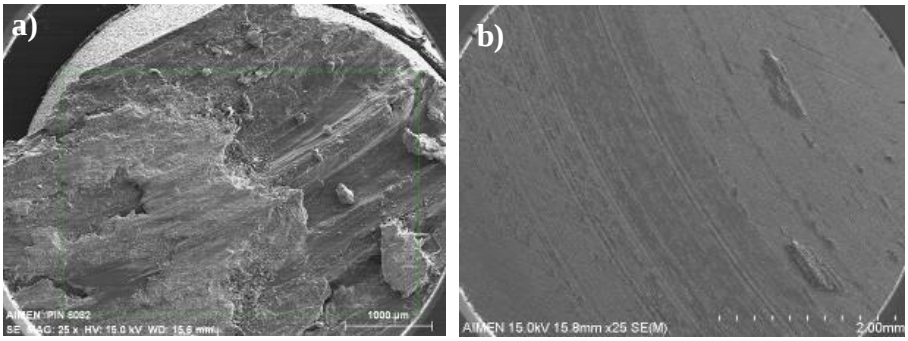

Figure 9. SEM micrographs of a) the worn surface of the 6082_C pin, and b) a detail of the wear track on the steel showing adhered aluminum and little grooves

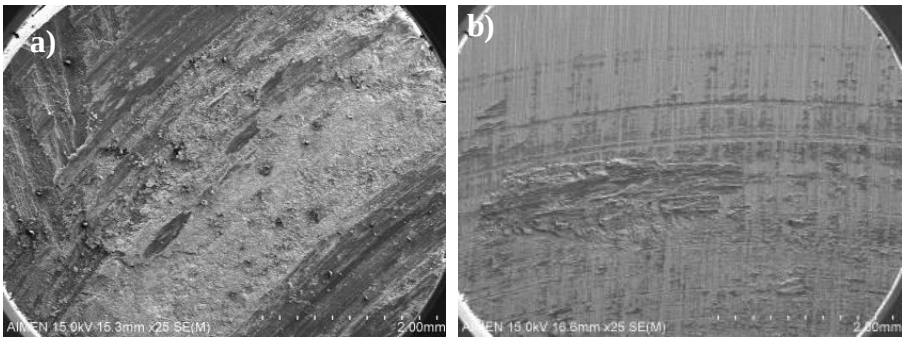

Figure 10. SEM micrographs of a) the worn surface of the 6061/Al_2O_3/10p_C pin, and b) of the wear track on the steel showing more adhered reinforced aluminum and deeper grooves

CONCLUSIONS

Extruded profiles of aluminum matrix composites with good surface and dimensional quality were produced on a 300 ton lab press.

The processing of AMCs profiles by extrusion requires higher press capacity than for the corresponding monolithic matrix alloys. The general trend is that maximum pressure increases in the following order (by profile): bar, T, L and U, and tube; and as volume fraction of reinforcement increases. In general, cast materials are easier to extrude than PM ones and $MoSi_2$ reinforced AMCs are easier to extrude than Al_2O_3 reinforced AMCs.

AMCs processed by powder metallurgy have significantly higher hardness than the monolithic alloys. Comparison between the intermetallic reinforced AMC, 6061/$MoSi_2$/25p_PM, and the corresponding unreinforced matrix alloy shows an increase in hardness of almost three times in the as-solutionized

condition and of more than 45% in the T6 condition. In addition, the PM composites do not need a heat treatment to acquire maximum hardness.

By adding reinforcing particles to aluminum, a significant increase in tensile strength and stiffness occur. The high tensile strength and modulus of the present PM composites, without decrease in specific properties, makes these AMCs interesting for structural applications.

Wear tests of 6082_C and 6061/Al_2O_3/10p_C pins show that adhesive and abrasive mechanisms were acting. Both aluminum and reinforced aluminum appeared adhered on the steel surfaces, also steel debris appeared adhered on the pin surfaces.

Acknowledgements

Spanish project TRACE2009_0251 from MICINN, Spain, and EXTRUGASA, Galicia, Spain, are gratefully acknowledged. Thanks are also due to Amalia San Román and Miguel Acedo for their help with the experimental work.

REFERENCES

Boey FYC. Yuan Z. Khor KA. Mechanical alloying for the effective dispersion of sub-micron SiCp reinforcements in Al–Li alloy composite. Mater Sci EngA 1998;252:276–287.

Borrego A, Fernández R, Cristina MC, Ibáñez J, González-Doncel G. Influence of extrusion temperature on the microstructure and the texture of 6061Al-15 vol.% SiCw PM composites. Comp Sci Tech 2002;62:731-742.

Chawla N. Chawla KK. Metal Matrix Composites. Springer. 2006.

Corrochano J. Lieblich M. Ibáñez J. On the role of matrix grain size and particulate reinforcement on the hardness of powder metallurgy Al–Mg–Si/$MoSi_2$ composites. Comp. Sci. Tech. 2009;69;1818-1824.

Corrochano J. Walker J.C. Lieblich M. Ibáñez J. Rainforth W.M. Dry sliding wear behaviour of powder metallurgy Al-Mg-Si alloy-$MoSi_2$ composites and the relationship with the microstructure. Wear 2011;270;658–665.

bis Corrochano J. Lieblich M. Ibáñez J. The effect of ball milling on the microstructure of powder metallurgy aluminium matrix composites reinforced with $MoSi_2$ intermetallic particles. Composites: Part A 2011;42;1093–1099.

Clyne TW. Withers PJ. An Introduction to Metal Matrix Composites. Cambridge University Press. 1993.

Fogagnolo JB. Robert MH. Torralba JM. Mechanically alloyed AlN particle-reinforced Al-6061 matrix composites: Powder processing. consolidation and mechanical strength and hardness of the as-extruded materials. Mater Sci EngA 2006;426:85–94.

Lieblich. M. González-Doncel G. Adeva. P. Ibáñez. J. Torralba M. Caruana G. Extrudability of PM 2124/SiCp aluminum matrix composite. J. Mater. Sci. Letters. 1997;16 ;726-728.

Liu YB. Kwok JKM. Lim SC. Lu L. Lai MO. Fabrication of A1-4.5Cu/15SiCp composites: I. Processing using mechanical alloying. J Mater Proc Tech 1993;37:441-451.

Lu L. Lai MO. Gupta M. Chua BW. Osman A. Improvement of microstructure and mechanical properties of AZ91/SiC composite by mechanical alloying. J Mater Sci 2000;35:5553-5561.

Lu L. Lai MO. Ng CW. Enhanced mechanical properties of an Al based metal matrix composite prepared using mechanical alloying. Mater Sci EngA 1998;252:203-211.

Murphy AM. Howard SJ. Clyne TW. Characterisation of severity of particle clustering and its effect on fracture of particulate MMCs. Mater Sci Tech 1998;14:959-968.

Ozdemir I. Ahrensb S. Mücklich S. Wielageb B. Nanocrystalline Al–Al_2O_3p and SiCp composites produced by high-energy ball milling. J Mater Proc Tech 2008;205:111–118.

Parvin N. Assadifard R. Safarzadeh P. Sheibani S. Marashi P. Preparation and mechanical properties of SiC-reinforced Al6061 composite by mechanical alloying. Mater Sci EngA 2008;492:134-140.

Prabhu B. Suryanarayana C. Ana.L. Vaidyanathan R. Synthesis and characterization of high volume fraction Al–Al_2O_3 nanocomposite powders by high-energy milling. Mater Sci EngA 2006;425:192–200.

Prasad SV. Asthana R. Aluminum metal–matrix composites for automotive applications: tribological considerations. Tribology Letters 2004;17(3):445-453.

Tan MJ. Zhang X. Powder metal matrix composites: selection and processing. Mater Sci EngA 1998;244:80-85.

Zebarjad SM. Sajjadi SA. Dependency of physical and mechanical properties of mechanical alloyed Al–Al2O3 composite on milling time. Materials and Design 2007;28:2113–2120.

Zhao N. Nashb P. Yang X. The effect of mechanical alloying on SiC distribution and the properties of 6061 aluminum composite. J Mater Proc Tech 2005;170:586-592.